Probing the "Two-Pronged Plug Two-Holed Socket" Model for the Mechanism of Binding of the Src SH2 Domain to Phosphotyrosyl Peptides: A Thermodynamic Study†

J. Michael Bradshaw,‡ Richard A. Grucza,‡ John E. Ladbury,§ and Gabriel Waksman*,‡

Department of Biochemistry and Molecular Biophysics, Washington University School of Medicine, Campus Box 8231, 660 South Euclid Avenue, St. Louis, Missouri 63110, and Department of Biochemistry and Molecular Biology, University College London, Gower Street, London WC1E 6BT, U.K.

Received December 23, 1997; Revised Manuscript Received April 24, 1998

ABSTRACT: Src homology 2 (SH2) domains are protein modules that specifically bind to tyrosyl phosphorylated peptides on signaling proteins. X-ray crystallographic studies of the SH2 domain of the Src kinase have probed the mechanism of binding, leading to the "two-pronged plug two-holed socket" mechanism whereby binding is hypothesized to resemble a two-pronged plug (the peptide) inserting into a two-holed socket (the SH2 domain). This binding model predicts (1) a hydrophobic basis for high-affinity binding largely determined by the level of insertion of the third residue C-terminal to the phosphotyrosine in the peptide into a primarily hydrophobic pocket (the +3 binding pocket) of the SH2 domain, and (2) a binding mechanism involving no significant conformational changes in the SH2 domain. In this study, we have probed these predictions by using isothermal titration calorimetry to extract complete thermodynamic profiles ($\Delta G°$, $\Delta H°$, $\Delta S°$, $\Delta C_p°$) for the binding of the Src SH2 domain to two series of tyrosyl phosphopeptides. One series consisted of peptides that have been determined by X-ray crystallography to have different levels of insertion of the peptide's +3 position into the +3 binding pocket. The other series consisted of peptides with progressively smaller hydrophobic side chains (I, L, V, and A) at the +3 position. Consistent with a binding mechanism that does not involve substantial conformational changes, the $\Delta C_p°$ values for all peptides were small and, at least for the high-affinity interactions, similar to the $\Delta C_p°$ values predicted from surface area calculations. However, unexpectedly, this study reveals that high-affinity binding was only partially determined by the interactions between the +3 residue in the peptide and the +3 binding pocket. Furthermore, the $\Delta C_p°$ values for all peptides studied were similar, implying similar degrees of desolvation of the +3 binding pocket upon binding. These results indicate that the "two-pronged plug two-holed socket" model is an oversimplification of the Src SH2 domain binding mechanism.

Src homology 2 (SH2) domains are ∼100 amino acid protein modules involved in signaling downstream of cell-surface receptors (*1*, *2*). Their function is to specifically bind tyrosine-phosphorylated sequences in target proteins. High-affinity SH2 domain binding is primarily mediated by the three to five amino acid residues in the target that are C-terminal to the phosphotyrosine (*3*). Due to this selectivity, SH2 domains have been and continue to be actively pursued as potential targets for pharmaceuticals (*4*).

The SH2 domain of the Src kinase has been extensively studied as one model for SH2 domain recognition. The structure of the Src SH2 domain has been determined in several forms including (1) a complex with a low-affinity peptide based on the platelet-derived growth factor receptor (PDGFR) (*5*), (2) a complex with a high affinity peptide based on the hamster middle T antigen (hmT) (*6*), (3) a complex with the C-terminal tail of Src (*7*), and (4) a peptide-free form (albeit phosphate-bound) (*6*). These structures showed several common features. In each of the SH2 domain−phosphopeptide complexes, the phosphotyrosine is bound within a positively charged cavity of the SH2 domain formed by the αA helix, the βB and βD strands, and the BC loop (Figure 1). In addition, the backbone structures of the peptide-free and peptide-bound SH2 domains are nearly invariant. However, the structure of the Src SH2 domain in complex with the hmT peptide shows an important feature not observed in the other structures: the presence of a hydrophobic or +3 binding pocket formed by the αB helix, βD strand, and EF and BG loops into which an Ile residue at the +3 position C-terminal to the phosphotyrosine in the ligand is inserted (Figure 1) (*6*). These structural studies prompted the "two-pronged plug two-holed socket" model, which proposed that (1) SH2 domain target recognition occurs through a rigid-body binding mechanism and (2) occupation of the +3 binding pocket by a large hydrophobic residue is important for high-affinity binding (*6*).

† This work was supported by funds from Washington University School of Medicine. J.E.L. is a Wellcome Trust Career Development Fellow.

* Corresponding author: Tel (314) 362-4562; Fax (314) 362-7183; E-mail waksman@gwiris1.wustl.edu.

‡ Washington University School of Medicine.

§ University College London.

S0006-2960(97)03147-4 CCC: $15.00
Published on Web 06/05/1998

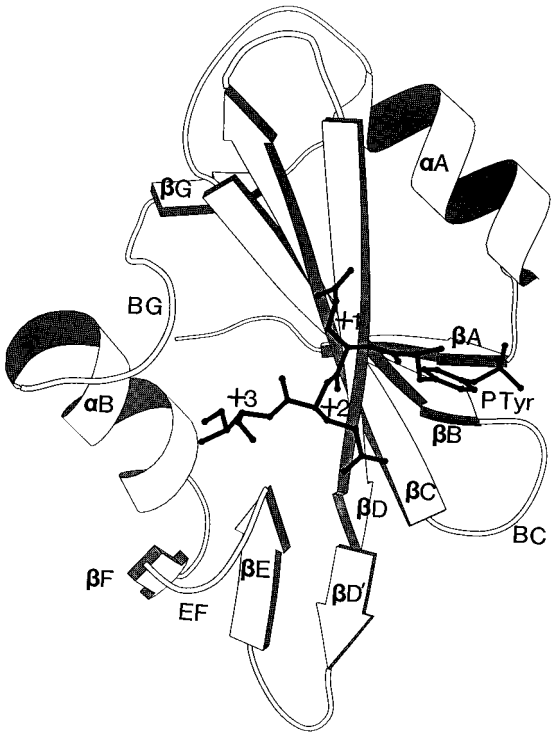

FIGURE 1: Schematic ribbon diagram of an SH2 domain. The structure shown is the Src SH2 domain complexed with hmT phosphopeptide (*6*). The α-helices, *β*-sheets, and loops of the SH2 domain are depicted as ribbons, arrows, and single lines, respectively. The notation used to label the secondary structure elements is that of *39*. The phosphotyrosine (pTyr), glutamate (+1), glutamate (+2), and isoleucine (+3) of the hmT peptide are also shown and labeled with black solid bonds.

Several studies have supported the "two-pronged plug two-holed socket" model. For example, a phosphopeptide library screen identified that the Src family of SH2 domains had selectivity for a hydrophobic amino acid side chain at the +3 position (*8*). In addition, mutations in the +3 binding pocket of the Src SH2 domain result in changes in peptide binding specificity, suggesting that specificity may be determined by regions of the SH2 domain structure that participate in forming this pocket (*9*, *10*). However, recent investigations indicate that the +3 binding pocket may not be the only site important for high-affinity binding. Replacing either the +1 or +2 residue within the consensus Glu-Glu-Ile motif of the hmT peptide with glycine caused a greater than 10-fold reduction in affinity for the homologous Lck SH2 domain (*11*, *12*), indicating that additional residues besides the +3 position are important for high-affinity binding. Furthermore, the binding of peptides based on the hmT peptide with nonconservative substitutions in the +3 position did not show dramatic decreases in affinity (*13*).

Additional information regarding a molecular recognition event can be obtained through the thermodynamics of the binding process, and SH2 domains have been the target of several calorimetric investigations (*14*−*19*). A thermodynamic approach should aid in the evaluation of the "two-pronged plug two-holed socket" model of SH2 domain recognition since the predictions of the model have specific thermodynamic signatures. For instance, if high-affinity SH2 domain recognition is determined by hydrophobic interactions in the +3 binding pocket, this will likely be reflected in a more negative ΔC_p° for high-affinity SH2 domain ligands. Likewise, if binding occurs with little conformational change in the SH2 domain, this should be reflected in a modest value of ΔC_p°.

We have therefore used isothermal titration calorimetry to obtain a complete thermodynamic characterization of the interaction of the Src SH2 domain with several phosphopeptides. Three of the six employed peptides (hmT, PDGFR, and C-tail) are based on potential physiological ligands of Src and were chosen on the basis of the different extents to which each peptide interacts with the +3 binding pocket of the SH2 domain [as determined by the X-ray crystallographic studies of Waksman et al. (*5*, *6*) and Xu et al. (*7*)]: the +3 Ile of the hmT peptide inserts fully into the hydrophobic binding pocket, the +3 Met of the PDGFR peptide inserts partially into the +3 pocket, and the +3 Gly of the low-affinity C-terminal tail peptide is incapable of interacting with the hydrophobic pocket. The remaining three peptides were based on the hmT peptide sequence with the +3 position systematically substituted to residues with smaller hydrophobic side chains (Leu, Val, or Ala). The thermodynamic characterization of these peptides surprisingly showed that (1) peptides with smaller hydrophobic side chains at the +3 position showed only moderately reduced binding affinity, (2) ΔC_p°, the thermodynamic parameter most reflective of hydrophobic interactions, was very similar for each peptide, and (3) the thermodynamic parameter that most distinguished high- versus low-affinity binding was ΔH°. Hence our data suggest that the "two-pronged plug two-holed socket" model may be an oversimplification of the true binding mechanism of the Src family of SH2 domains.

MATERIALS AND METHODS

Protein Expression and Purification. The Src SH2 domain was expressed and purified as described by Waksman et al. (*5*). The resulting material was then applied to a HiPrep Sephacryl 26/60 S-100 gel-filtration column preequilibrated in 20 mM MES, pH 6.0, 1 mM *β*-mercaptoethanol, 1 mM EDTA, and 50 mM NaCl. Src SH2 domain purity was assessed to be >98% by SDS−PAGE. The protein was further dialyzed against a standard calorimetry buffer prior to titrations (see below). An extinction coefficient for the Src SH2 domain of $\epsilon_{280} = 14\,700\ M^{-1}\ cm^{-1}$ was obtained by the Edelhoch method (*20*, *21*).

Tyrosine Phosphopeptides. Tyrosine phosphorylated peptides were obtained from Quality Controlled Biochemicals (Hopkinton, MA). The following peptides were employed in this study: (1) Ac-PQ(pY)EEIPI-NH_2, derived from the hamster middle T antigen (hmT) (*6*), (2) Ac-TQ(pY)-VPMLE-NH_2, derived from residues 749−756 of the *β*-subunit of the human platelet-derived growth factor receptor (PDGFR), and (3) Ac-PQ(pY)QPGEN-NH_2, derived from residues 525−532 of the regulatory tail of human Src (C-tail). The hmT peptide variants had a sequence identical to the hmT peptide except for the noted changes at the +3 position. Estimates of peptide concentration were obtained both by mass and by using an extinction coefficient obtained by quantitative amino acid analysis. Peptides were dialyzed into the standard buffer using a Pierce Microdialyzer before calorimetry experiments in order to remove excess salts that remained after peptide synthesis.

Analytical Ultracentrifugation and Dynamic Light Scattering. Recent studies have shown that the SH2 domains of both the Src homologous and collagen-like protein (SHC) and the fyn tyrosine kinase can dimerize in solution (*22*, *23*). However, high-speed sedimentation equilibrium experiments, performed as previously described with a Beckman XL-A Optima analytical ultracentrifuge (*22*), indicated that the Src SH2 domain was monomeric. Sedimentation experiments were performed in several different buffers (20 mM sodium acetate, pH 5.2; 20 mM MES, pH 6.0; 20 mM MOPS, pH 6.8; 20 mM Hepes, pH 7.5; or 20 mM Tris, pH 9.0; all buffers containing in addition 50 mM NaCl, 1 mM β-mercaptoethanol, and 1 mM EDTA) and the experiments in 20 mM MES, pH 6.0, gave the best fit to a single species model, so subsequent calorimetry experiments were performed at pH 6.0. The monomeric state of assembly was further confirmed with dynamic light scattering experiments, performed with a DynaPro-801 dynamic light scattering instrument (Proteins Solutions, Ltd.), which indicated that the Src SH2 domain, either alone or complexed with either a hmT, PDGFR, or C-terminal tail phophopeptide, did not dimerize up to a concentration of 500 μM.

Isothermal Titration Calorimetry. Calorimetry experiments were performed with an Omega titration calorimeter obtained from Microcal, Inc. (Northhampton, MA) (*24*). Solutions were degassed for 15−30 min under vacuum prior to experiments. The standard buffer for the calorimetry experiments was 20 mM MES, pH 6.0, 1 mM β-mercaptoethanol, 1 mM EDTA, and 50 mM NaCl. The experiments in buffers other than the standard buffer each contained 20 mM buffer (sodium cacodylate, ACES, Bistris, sodium citrate), 1 mM β-mercaptoethanol, 1 mM EDTA, and 50 mM NaCl. The heat of ionization at 25 °C for each of the buffers was obtained from the literature (*25*, *26*) (MES, 3730 cal mol^{-1} deg^{-1}; sodium cacodylate, −560 cal mol^{-1} deg^{-1}; ACES, 7470 cal mol^{-1} deg^{-1}; Bistris, 6750 cal mol^{-1} deg^{-1}; sodium citrate, −800 cal mol^{-1} deg^{-1}). Corrections were incorporated for the change in the heat of ionization with temperature for the MES and sodium citrate buffers (*25*).

For a typical titration of Src SH2 domain with the hmT peptide or hmT peptide variants, 50−100 μM Src SH2 domain was placed in the 1.35 mL reaction cell while 1.0−2.0 mM phosphopeptide was loaded into the 250 μL injection syringe. The lower affinity of the PDGFR and C-terminal tail peptides dictated that higher concentrations of protein and peptide be employed. For these experiments, 150−400 μM Src SH2 domain was titrated with either 5 or 10 μL injections of 3.5−4.0 mM peptide. The *c* value, defined by Wiseman et al. (*24*) to be the product of the association constant for the reaction, *K*, and the macromolecule concentration, *M*, varied from 100 to 500, from 20 to 50, or from 4 to 14 for the experiments in MES buffer employing the hmT (or variants thereof), PDGFR, or C-tail phosphopeptides, respectively. The *c* values of experiments employing the hmT and PDGFR peptide in sodium citrate buffer varied from 20 to 50 and from 3 to 5, respectively, while the *c* value of the C-tail peptide in sodium citrate was below the range of $c = 1-1000$ for which an accurate binding constant can be obtained. All values reported in the Results section are the result of at least three independent titration experiments.

Analysis of Calorimetric Data. The data for each titration was collected by the Origin software. The heats of injection were then fit to a version of the single-site binding model by employing a nonlinear least-squares algorithm (Marquardt method) using Scientist (Micromath, Salt Lake City, UT). The employed model, based on that originally described by Wiseman et al. (*24*), accounts for a nonzero upper baseline after saturation of all macromolecule binding sites. This was found to be occasionally necessary when the values of the heats of each injection after the protein had been saturated with peptide were not identically represented by control experiments where peptide was injected into buffer alone. Multiple titrations performed under the same conditions were analyzed simultaneously in order to provide a single best-fit value for each fitted parameter. In general, varying the peptide concentration during the fitting procedure while holding the stoichiometry fixed at $n = 1$ provided a better fit to multiple titrations than fixing the peptide concentration and varying the stoichiometry, *n*. The uncertainties in fitted parameters represent 95% support plane confidence intervals.

Calculation of Accessible Surface Areas. Accessible surface area (ASA) calculations were performed using TINKER (Dr. Jay Ponder, Washington University), which employs an algorithm by Richmond (*27*) that has been modified by Wesson and Eisenberg (*28*). A 1.4 Å probe radius was employed. The structures used in this study have the following entry numbers in the Brookhaven Protein Data Base: Src SH2−PDGFR (1SHA), Src SH2−hmT (1SPS), and peptide-free Src SH2 (1SPR). The coordinates of the complex of Src with the C-terminal tail were a generous gift of Dr. Michael Eck (Harvard University).

To calculate the change in accessible surface area (ΔASA) upon peptide binding, the polar and nonpolar surface areas of the free Src SH2 domain (ASA_{SH2}), free peptide ($ASA_{peptide}$), and Src SH2 domain−peptide complex ($ASA_{SH2+peptide}$) were determined for each peptide studied. The change in either polar or nonpolar accessible surface area was then computed from

$$\Delta ASA = ASA_{SH2+peptide} - (ASA_{SH2} + ASA_{peptide}) \quad (1)$$

The $ASA_{SH2+peptide}$ was calculated from each of the three Src SH2 domain−peptide crystal structures studied, while ASA_{SH2} was determined from the peptide-free Src SH2 domain crystal structure. $ASA_{peptide}$ was calculated as the sum of the accessible surface areas of the individual residues in the extended Ala-X-Ala geometry ($ASA_{tripeptide}$) (*29*, *30*).

The Src SH2 domain−PDGFR peptide structure contained only a five-residue peptide, while an octapeptide was used in the calorimetric studies. To obtain accurate surface area calculations, the −1 (Q) and −2 (T) positions of the PDGFR peptide were modeled with the program MACROMODEL (Clark Still, Columbia University). The positions of these residues were based on the positions of the corresponding residues in the hmT crystal structure. After the addition of these residues, a simple energy minimization was performed to dock the newly added residues against the Src SH2 domain and surface area calculations were then performed.

RESULTS

Thermodynamic Parameters of Binding of the hmT, PDGFR, and C-Tail Phosphopeptides to the Src SH2 Domain.

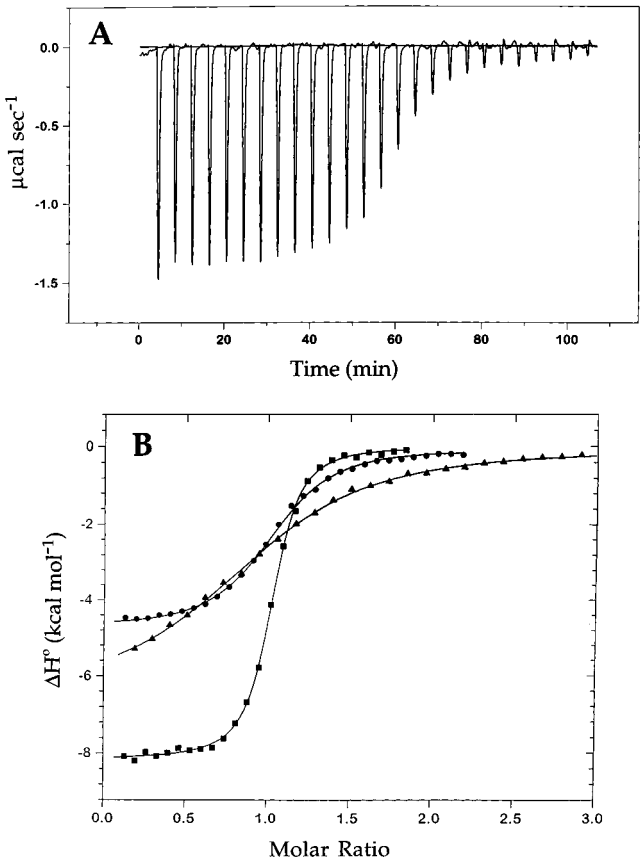

FIGURE 2: Isothermal calorimetric titrations for binding of the Src SH2 domain to the hmT, PDGFR, and C-tail tyrosyl-phosphorylated peptides. (A) Raw heat signal of an isothermal titration of the Src SH2 domain with the hmT phosphopeptide. The power output (microcalories per second) is shown as a function of time (minutes). This experiment was performed at 25 °C and consisted of 26 × 5 μL injections of 1.14 mM phosphopeptide into the 1.35 mL reaction cell containing 61 μM Src SH2 domain. (B) Integrated data for titrations of the hmT (■), PDGFR (●), and C-terminal tail (▲) phosphopeptide with the Src SH2 domain. Integrated data are obtained from the raw heat signal as described in the Materials and Methods section. The solid line through each set of data represents the nonlinear least-squares best fit to the data. All titrations shown here were performed at 25 °C in 20 mM MES, pH 6.0, 1 mM β-mercaptoethanol, 1 mM EDTA, and 50 mM NaCl.

Isothermal titration calorimetry is a technique that allows a simultaneous determination of the association constant (K) of a reaction as well as the enthalpy of binding ($\Delta H°$). From these parameters, the Gibbs free energy ($\Delta G°$) and the entropy of binding ($\Delta S°$) can be derived from the expressions $\Delta G° = -RT \ln K$ and $T\Delta S° = \Delta H° - \Delta G°$. Figure 2A shows raw data from a titration of the Src SH2 domain with the hmT peptide at 25 °C, while Figure 2B displays representative integrated data from titrations of the Src SH2 domain with the hmT, PDGFR, and C-terminal tail phosphopeptides. The association constants (K) and enthalpies ($\Delta H°$) for each peptide in MES buffer at 25 °C are shown in Table 1. The hmT peptide binds with the highest relative affinity ($K = 5 \times 10^6$ M^{-1} or $K_d = 200$ nM), while the PDGFR and C-terminal tail peptides bind with intermediate ($K_d = 5.9\ \mu$M) and low ($K_d = 29.4\ \mu$M) affinity, respectively. The binding constant values for the three peptides confirm previous studies, which showed that the difference between high- and low-affinity binding to SH2 domains is ~2 orders of magnitude or less (*16, 31*).

Table 1: Calorimetric Data for Src SH2 Domain Binding to Phosphopeptides

peptide	K^a (M^{-1})	$\Delta H°$ [a] (kcal mol^{-1})
	hmT	
MES	5 (± 2) × 10^6	−8.4 ± 0.7
ACES	6 (± 3) × 10^6	−10.3 ± 0.9
cacodylate	3 (± 2) × 10^6	−6.2 ± 0.8
bistris	6 (± 3) × 10^6	−10.4 ± 0.3
citrate	2.4 (± 0.4) × 10^5	−7.6 ± 0.5
	PDGFR	
MES	1.7 (± 0.3) × 10^5	−4.5 ± 0.1
ACES	2.5 (± 0.4) × 10^5	−5.6 ± 0.2
cacodylate	1.2 (± 0.3) × 10^5	−3.2 ± 0.1
citrate	6.4 (± 0.8) × 10^3	−3.3 ± 0.8
	C-Tail	
MES	3.4 (± 0.4) × 10^4	−5.8 ± 0.2
ACES	4.9 (± 0.4) × 10^4	−7.1 ± 0.2
cacodylate	2.1 (± 0.4) × 10^4	−4.6 ± 0.1

[a] Uncertainties represent 1 standard deviation of multiple experiments. Each experiment was performed in 20 mM buffer, 1 mM β-mercaptoethanol, 1 mM EDTA, and 50 mM NaCl, pH 6.

The measured enthalpy ($\Delta H°$) in a calorimetry experiment is the composite heat of many processes including the enthalpy of ligand binding ($\Delta H°_o$) as well as the enthalpy of protonation/deprotonation of the employed buffer. Effects of buffer ionization are corrected by performing calorimetry experiments in different buffers with different heats of ionization ($\Delta H°_{ion}$) and calculating $\Delta H°_o$ from the expression

$$\Delta H° = \Delta H°_o + n\Delta H°_{ion} \quad (2)$$

where n is the number of protons exchanged with the buffer. Table 1 shows the association constants (K) and measured enthalpies ($\Delta H°$) for the binding of the hmT, C-tail, and PDGFR peptides to the Src SH2 domain in several different buffers with different $\Delta H°_{ion}$. For all three peptides, the choice of buffer (except sodium citrate, see below) has little effect on the binding constant. However, the measured enthalpy $\Delta H°$ is strongly affected by the buffer. A plot of $\Delta H°$ vs $\Delta H°_{ion}$ for each peptide shows a decreasing trend for all peptides, indicating an uptake of protons by the buffer (Figure 3). From this plot, the number of protons exchanged (n) for all three peptides was determined [n(hmT) = −0.5 ± 0.2, n(PDGFR) = −0.3 ± 0.1, n(C-tail) = −0.3 ± 0.1] (Table 2). Recent data suggest that the proton release which occurs upon peptide binding is likely derived from the phosphate group of the phosphotyrosine (Bradshaw and Waksman, manuscript in preparation).

The association constants of both the hmT and PDGFR peptides are reduced ~20-fold when the calorimetry experiments are performed in sodium citrate buffer (the C-tail association constant is too low to be measured in sodium citrate). It is likely that this effect at least partially results from the high negative charge of the citrate ion, which gives the solution a higher ionic strength than the other employed buffers. It is also possible that citrate could specifically interact with the SH2 domain and inhibit peptide binding. In either case, further experiments are necessary to fully define the role citrate plays in Src SH2 domain target recognition. However, the similar magnitude of decreased affinity (~20-fold) of the hmT and PDGFR peptides suggests that the effect of citrate is not specific for a particular peptide.

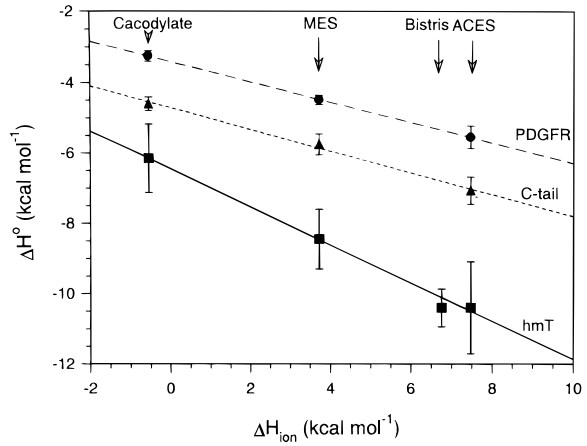

FIGURE 3: Enthalpies of binding for the Src SH2 domain binding to the hmT (■), PDGFR (●), and C-terminal tail (▲) phosphopeptides as a function of the $\Delta H°_{ion}$ of the buffer. Error bars on the enthalpy value represent the standard deviation of multiple experiments. A linear least-squares best fit of the hmT (solid line), PDGFR (dashed line), and C-terminal tail (dotted line) enthalpy values gives the number of protons exchanged with the buffer, *n*, upon binding. The uncertainty in the value of *n* represents a 67% confidence interval on the best linear fit.

The enthalpy ($\Delta H°_o$), corrected for buffer effects, and the entropy ($T\Delta S°$) of peptide binding to the Src SH2 domain at 25 °C are listed in Table 2. The binding of all three peptides (hmT, PDGFR, and C-tail) occurred with a favorable $\Delta H°_o$ as has been seen previously for SH2 domain−phosphopeptide interactions (*14*−*16*), with $T\Delta S°$ for each peptide also contributing favorably to $\Delta G°$ at 25 °C. A comparison of the binding energetics of the hmT and PDGFR peptides reveals that the hmT peptide has a much larger binding enthalpy ($\Delta\Delta H°_o = 3.1$ kcal mol^{-1}) but a less favorable entropy ($T\Delta\Delta S° = 1.1$ kcal mol^{-1}). In contrast, binding of the hmT peptide is more energetically favorable than that of the C-tail peptide due to more favorable contributions from both the enthalpy ($\Delta\Delta H°_o = 1.9$ kcal mol^{-1}) and entropy ($T\Delta\Delta S° = -1.0$ kcal mol^{-1}) of binding. However, in both cases, the Src SH2 domain binds the hmT peptide with greater affinity largely due to an at least ∼2 kcal mol^{-1} more favorable $\Delta H°_o$.

Finally, since the corrected values for enthalpies of binding reported here are the first such values ever reported for SH2 domains of the Src family of proteins, we are not in a position to compare these values with binding enthalpies reported elsewhere.

Temperature Dependence of Thermodynamic Parameters for Binding of the hmT, PDGFR, and C-Tail Phosphopeptides to the Src SH2 Domain and Surface Area Calculations. Calorimetry experiments in MES buffer were performed in 5° intervals from 10 to 40 °C, and the $\Delta H°_o$ values from these experiments are plotted in Figure 4A. The binding enthalpies were negative at all temperatures examined, and the decreasing enthalpy trend of each peptide fit well to a linear function, whose slope gave the heat capacity change ($\Delta C_p°$) upon binding that peptide to the SH2 domain. The $\Delta C_p°$ of each peptide was modest (between −150 and −220 cal mol^{-1} deg^{-1}), which is indicative of a rigid-body interaction that does not involve any significant conformational changes in the protein (*32*). These results are consistent with the crystallographic studies of the bound and unbound states of the Src SH2 domain, which show only limited conformational changes between these two states (*6*). The heat capacity changes of the hmT and PDGFR peptides were very similar in magnitude [$\Delta C_p°$ (hmT) = −196 ± 25 cal mol^{-1} deg^{-1}; $\Delta C_p°$ (PDGFR) = −212 ± 17 cal mol^{-1} deg^{-1}], with the $\Delta C_p°$ of the C-tail ∼20% smaller [$\Delta C_p°$ (C-tail) = −159 ± 28 cal mol^{-1} deg^{-1}]. Hence, $\Delta C_p°$ does not correlate either with the extent of hydrophobic contacts between the peptides and the SH2 domain or with the extent of insertion of the +3 peptide residue within the +3 binding pocket of the SH2 domain (See introduction and surface area calculations below).

Given the dramatic effect of the sodium citrate buffer on peptide binding affinities at 25 °C, we speculated that sodium citrate might also have an effect on the $\Delta C_p°$ of peptide binding and hence alter our conclusions regarding the role of hydrophobic interactions in the binding process. However, a value of $\Delta C_p°$ (hmT) = −176 ± 25 cal mol^{-1} deg^{-1} was determined in sodium citrate buffer, which is only slightly smaller than the $\Delta C_p°$ obtained in MES buffer. Hence, sodium citrate does not affect the $\Delta C_p°$.

Figure 4B shows the Gibbs free energy as a function of temperature for each peptide. For all peptides, $\Delta G°$ is relatively invariant with temperature. Hence the hmT peptide binds ∼2 kcal mol^{-1} and ∼2.9 kcal mol^{-1} more favorably than the PDGFR and C-terminal tail peptides, respectively, over the entire temperature range studied. Since $\Delta G°$ is constant as a function of temperature, the $T\Delta S°$ of binding decreases with increasing temperature. Hence, $\Delta H°_o$ and $\Delta S°$ compensate to provide a relatively constant $\Delta G°$.

To probe the extent to which hydrophobic interations contribute to Src SH2 domain binding, nonpolar and polar surface area calculations were performed on each of the Src SH2 domain structures. We found that the hmT, PDGFR, and C-tail peptides bury 1067, 968, and 782 Å^2, respectively, of total surface area upon binding (Table 3). However, the striking result of these calculations is that the hmT peptide buries over 200 Å^2 more nonpolar surface than either the PDGFR or C-tail phosphopeptide. Hence, the extensive interactions between the +3 Ile of the hmT phosphopeptide and the hydrophobic pocket of the SH2 domain are reflected in the amount of total nonpolar buried surface upon binding the hmT peptide.

Expressions that relate the change in nonpolar and polar surface area to $\Delta C_p°$ have been formulated (*32*, *33*), and Table 3 compares the $\Delta C_p°$ predicted on the basis of one of these expressions to the experimental $\Delta C_p°$. Due to the large change in nonpolar surface area, the hmT peptide was predicted to bind with a significantly more negative $\Delta C_p°$ than the PDGFR and C-tail peptides. However, the experimental $\Delta C_p°$ values for the PDGFR and C-tail peptides are much larger than anticipated by the surface area calculations. Although it is not the focus of this study to evaluate the correlation between $\Delta C_p°$ and the change in surface area, it is worth mentioning several plausible explanations for the lack of quantitative correlation between the predicted and experimental $\Delta C_p°$ for the PDGFR and C-tail peptides: (1) the hmT peptide buries 63% nonpolar surface area, while only 48% and 47% of the PDGFR and C-tail peptides' buried surface is nonpolar; since the average amount of hydrophobic surface area buried during protein folding is 59% (*32*), the predictions of $\Delta C_p°$ may be inaccurate for the PDGFR and C-tail peptides since they bury a much lower percentage of

Table 2: Thermodynamic Parameters of Src SH2 Domain Binding to Phosphopeptides

peptide	K^a (M^{-1})	$\Delta G°$ [b] (kcal mol^{-1})	$\Delta H°_o$ [c] (kcal mol^{-1})	$T\Delta S°$ [d] (kcal mol^{-1})	$\Delta C_p°$ [e] (cal mol^{-1} $°C^{-1}$)	n^f
hmT	$5 (\pm 2) \times 10^6$	-9.1 ± 0.3	-6.5 ± 0.5	2.6 ± 0.6	-196 ± 25	0.5 ± 0.2
PDGFR	$1.7 (\pm 0.3) \times 10^5$	-7.1 ± 0.2	-3.4 ± 0.2	3.7 ± 0.3	-212 ± 17	0.3 ± 0.1
C-tail	$3.4 (\pm 0.4) \times 10^4$	-6.2 ± 0.4	-4.6 ± 0.3	1.6 ± 0.5	-159 ± 28	0.3 ± 0.1

[a] Taken from experiments in MES buffer. [b] Calculated from $\Delta G° = -RT \ln K$. [c] Determined from Figure 3. [d] Calculated from $T\Delta S° = \Delta H°_o - \Delta G°$. [e] Determined from Figure 4A. [f] Determined from Figure 3.

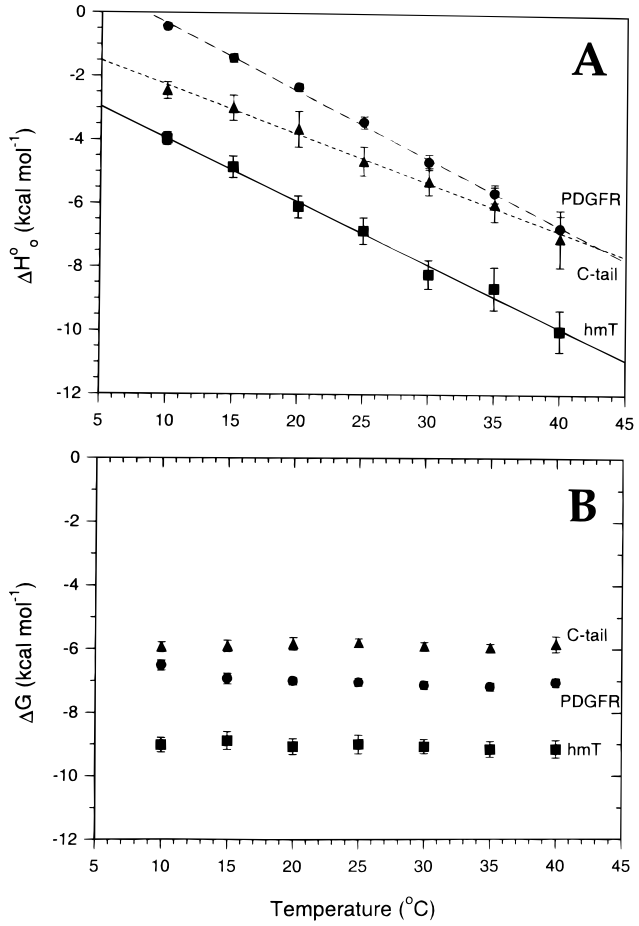

FIGURE 4: Temperature dependence of thermodynamic parameters for binding of the Src SH2 domain to tyrosyl-phosphorylated peptides. (A) Enthalpies of binding for the Src SH2 domain binding to the hmT (■), PDGFR (●), and C-terminal tail (▲) phosphopeptides as a function of temperature. Error bars on the enthalpy values represent 95% confidence intervals. A linear least-squares best fit of the hmT (solid line), PDGFR (dashed line), and C-terminal tail (dotted line) enthalpy values gives the heat capacity change for each peptide, which are listed in the text. The uncertainty in the heat capacity value represents a 95% confidence interval on the best linear fit. (B) Gibbs free energy of binding for the Src SH2 domain binding to the hmT (■), PDGFR (●), and C-terminal tail (▲) phosphopeptides as a function of temperature. Error bars on the free energy values represent 95% confidence intervals.

nonpolar surface area than is typical; (2) the interaction of peptides with the Src SH2 domain buries a relatively small amount of area compared to protein folding and many other protein−protein interactions, so the predictions for this system are intrinsically more uncertain; and (3) since an underestimate of $\Delta C_p°$ has been linked to coupled folding processes in other systems (*32*), it is possible that the PDGFR and C-tail peptides could undergo small changes in conformation upon binding to the SH2 domain.

Table 3: Calculated Nonpolar and Polar Surface Area Removed from Solvent and the Predicted $\Delta C_p°$

peptide	ΔA_{tot} [a] (Å^2)	ΔA_{np} [a] (Å^2)	ΔA_p [a] (Å^2)	$\Delta C_p°_{pred}$ [b] (cal mol^{-1} deg^{-1})	$\Delta C_p°_{exp}$ [c] (cal mol^{-1} deg^{-1})
hmT	1067	668	399	-197 ± 25	-196 ± 25
PDGFR	968	467	501	-80 ± 21	-212 ± 17
C-tail	782	369	413	-59 ± 15	-159 ± 28

[a] Determined from eq 1 in the text. [b] Calculated according to $\Delta C_p° = 0.45 (\pm 0.02)\ \Delta A_{np} - 0.26 (\pm 0.03)\ \Delta A_{pol}$ from Murphy and Freire (*33*). [c] Calculated from the linear best fit to the enthalpy as a function of temperature. The uncertainties represent 95% confidence intervals on the best fit.

Binding Energetics of hmT Peptide Variants. To specifically examine the interaction between the +3 position of the peptide and the hydrophobic binding pocket, the binding of a series of peptides based on the hmT peptide sequence with the +3 position systematically substituted to residues with smaller hydrophobic side chains (Ala, Val, and Leu) was examined (Table 4). In these peptides, the +3 Ile of the hmT peptide was changed to Leu, Val, and Ala. The Src SH2 domain binds peptides with Leu [hmT(I+3L)] and Val [hmT(I+3V)] at the +3 position with similar $\Delta G°$ as the hmT peptide, indicating that the +3 binding pocket of the Src SH2 domain is relatively insensitive to the hydrophobic residue present at the +3 position in the peptide. However, both of these peptides show a less favorable $\Delta H°$ compensated by a more favorable $T\Delta S°$, indicative of a loss of favorable van der Waals contacts (see Discussion). Substitution of Ile to Ala [hmT(I+3A)] results in a modest increase (1.0 kcal mol^{-1}) in $\Delta G°$, a substantially less favorable $\Delta H°$, and a slightly smaller $\Delta C_p°$ than the hmT peptide. The less favorable $\Delta H°$ observed for the hmT-(I+3A) peptide relative even to the hmT(I+3L) or hmT-(I+3V) peptide is particularly interesting and may reflect a complete loss of van der Waals contacts between the side chain of the +3 residue in the hmT(I+3A) peptide and the +3 binding pocket.

DISCUSSION

A knowledge of the energetics of high-affinity phosphopeptide recognition by SH2 domains will help facilitate an understanding of how SH2 domains mediate specificity in signal transduction events. As a first step toward this aim, we have used isothermal titration calorimetry to probe the model that has constituted the conceptual basis for Src-like SH2 domain target recognition: the "two-pronged plug two-holed socket" model. The most important findings of this study are (1) interactions at the +3 hydrophobic binding pocket of the SH2 domain only partially determine high-affinity binding and specificity, (2) no large "induced fit" type of conformational change occurs in the SH2 domain

Table 4: Thermodynamic Binding Parameters of hmT Peptides with Amino Acid Substitutions at the +3 Position[a]

peptide	K (M^{-1})	$\Delta G°$ (kcal/mol)	$\Delta H°$ (kcal/mol)	$\Delta C_p°$ [cal/(mol deg)]	$\Delta\Delta G°$ [b] (kcal/mol)	$\Delta\Delta H°$ [b] (kcal/mol)	$T\Delta\Delta S°$ [b] (kcal/mol)	$\Delta\Delta C_p°$ [b] [cal/(mol deg)]
hmT(I+3L)	$4 (\pm 0.6) \times 10^6$	-9.0 ± 0.1	-7.7 ± 0.1	nd[c]	0.1	0.7	0.6	nd[c]
hmT(I+3V)	$3 (\pm 0.9) \times 10^6$	-8.8 ± 0.2	-7.6 ± 0.3	nd[c]	0.3	0.8	0.5	nd[c]
hmT(I+3A)	$0.9 (\pm 0.1) \times 10^6$	-8.1 ± 0.1	-6.7 ± 0.2	-165 ± 10	1.0	1.7	0.7	31

[a] Experiments were performed in MES buffer at 25 °C. Uncertainties represent the standard deviation of multiple experiments. [b] Calculated in reference to the thermodynamic parameters for the hmT peptide in MES buffer (Table 1). The comparisons of $\Delta H°$ and $T\Delta S°$ assume that an identical release of protons occurs upon binding the hmT and hmT variant peptides. [c] Not determined.

upon binding, and (3) $\Delta H°_o$, not $\Delta S°$ nor $\Delta C_p°$, is the thermodynamic parameter that most distinguishes binding of the hmT peptide from the lower affinity peptides.

The "two-pronged plug two-holed socket" model of Src SH2 domain recognition, formulated on the basis of the crystal structures of the Src SH2 domain in complex with several peptide ligands (*5, 6*), proposed that the occupation of the +3 binding pocket by a hydrophobic residue at the peptide's +3 position was the critical determinant of high-affinity Src SH2 domain binding. Here we show that peptide binding affinity correlates well with the size of the hydrophobic side chain at the +3 position of the ligand, confirming that indeed the interactions between the peptide and the +3 binding pocket are important. However, the effects of various substitutions at the +3 position are modest, which suggests that the "two-pronged plug two-holed socket" model may be a somewhat simplistic model of peptide recognition by Src-like SH2 domains. In particular, the finding that a substitution to Ala at the +3 position of the hmT peptide only results in a small loss in binding free energy indicates that the +3 binding pocket contributes only partially to high-affinity binding and hence to the specificity of Src SH2 domain−phosphopeptide interactions.

The study presented here represents the first determination of the heat capacity changes upon binding of high- and low-affinity phosphopeptides to SH2 domains of the Src family of proteins. Somewhat surprisingly, the $\Delta C_p°$ values for each of the phosphopeptides studied were relatively similar, implying a relatively similar degree of desolvation of the protein and peptide surfaces upon binding. Both the surface area calculations (Table 3), as well the intimate contacts observed in the crystal structure between the +3 Ile of the hmT peptide and the +3 binding pocket of the SH2 domain, predicted the hmT peptide to have a $\Delta C_p°$ of binding more negative than the PDGFR and C-tail peptides. This was not the case, suggesting that high-affinity binding may not be determined solely by a potential hydrophobic effect at the +3 binding pocket. However, it should be noted that the $\Delta C_p°$ values of the C-tail and hmT(I+3A) peptides were ~20% smaller than the nearly identical $\Delta C_p°$ values of the hmT and PDGFR peptides. Although such a small difference in $\Delta C_p°$ may not be significant, it may nevertheless indicate a minor role for desolvation of the +3 binding pocket in the binding of the hmT and PDGFR peptides.

The values for the heat capacity change for all peptides were small and, at least for the high-affinity hmT peptide−SH2 domain interaction, very similar to the values predicted from surface area calculations. These observations are consistent with a binding mechanism that does not involve large conformational changes either in the SH2 domain or in the peptide. These results corroborate the crystallographic studies by Waksman et al. (*5, 6*) and are consistent with the "two-pronged plug two-holed socket" binding mechanism. However, the peptide-free structure of the Src SH2 domain actually represents a complex of the protein with phosphate bound within the phosphotyrosine-binding pocket: this leaves the possibility that the full extent of the conformational changes at the phosphotyrosine-binding site may not have been captured by the comparison of this structure with that of the SH2 domain−hmT peptide complex (*6*). Here, we provide the evidence that even in the absence of phosphate ion, only limited (if any) conformational changes occur upon binding.

Rather than $\Delta C_p°$, it was the relatively large $\Delta H°$ of binding for the hmT peptide that distinguished binding of the hmT peptides from the other peptides examined. The binding of even the conservatively substituted hmT peptide variants hmT(I+3L) and hmT(I+3V) showed a distinct loss in $\Delta H°$ compared to the hmT peptide. Because the magnitude of $\Delta C_p°$ of binding for all peptides is relatively similar, it is likely that the greater $\Delta H°$ observed for the high-affinity hmT peptide−Src SH2 domain interaction is largely the result of more favorable hydrogen bonding and van der Waals interactions (*34, 35*). The comparison of the Src SH2 domain−phosphopeptide crystal structures (Table 3) showed that the Src SH2 domain−hmT peptide complex is characterized by a greater contact surface area than the two lower affinity PDGFR and C-tail peptide−SH2 domain complexes, which is consistent with a greater number of van der Waals interactions and hence a more favorable $\Delta H°$ for the hmT peptide. Furthermore, the hmT peptide−Src SH2 domain structure also revealed the presence of an extensive water-mediated hydrogen-bonding network centered around the βD−DE loop−βE region of the SH2 domain that coordinates the +2 Glu position in the peptide, as well as several long-range interactions between Lys βD3 of the SH2 domain and the +1 Glu position. These interactions were not observed in the complexes of the Src SH2 domain with the PDGFR and C-tail peptides, which is consistent with a less favorable $\Delta H°$ for the binding of these peptides. Our thermodynamic analysis suggests that the hydrogen bonds (water-mediated or not) and van der Waals interactions observed between the hmT peptide and the SH2 domain are significant and may promote high-affinity binding.

The investigation presented here is limited to a class of SH2 domains that belong to the Src family of kinases. This class is characterized by a mode of binding that resembles a "two-pronged plug two-holed socket" interaction. Other SH2 domains, such as those of the phospholipase Cγ (PLCγ) and the adaptor protein Grb2, display different recognition surfaces. The PLCγ family of SH2 domains is characterized by a long hydrophobic groove interacting with the +3 and +5 positions of the peptide ligand (*36, 37*), while the Grb2 SH2 domain has Trp EF1 filling its hydrophobic pocket (*38*).

A thermodynamic characterization of Grb2 SH2 domain binding to its high-affinity peptide revealed many similarities with the Src SH2 domain−hmT peptide interaction: a similar $\Delta G°$, binding driven by a favorable $\Delta H°_o$, and a modest $\Delta C_p°$ (*18*). Further comparisons of the binding energetics of SH2 domains will provide further information about the nature of SH2 domain binding affinity.

ACKNOWLEDGMENT

We thank Drs. D. Cistola, G. K. Ackers, A. Vindigni, C. Clarke, and A. Kozlov for helpful comments on the manuscript and Drs. J. I. Gordon and R. S. Bhatnagar for the use of the Microcal calorimeter.

REFERENCES

1. Sadowski, I., Stone, J. C., and Pawson, T. (1986) *Mol. Cell. Biol. 6*, 4396−4408.
2. Cantley, L. C., Auger, K. R., Carpenter, C., Duckworth, B., Graziani, A., Kapeller, R., and Soltoff, S. (1991) *Cell 64*, 281−302.
3. Pawson, T., and Schlessinger, J. (1993) *Curr. Biol. 3*, 434−442.
4. Brugge, J. S. (1993) *Science 260*, 918−919.
5. Waksman, G., Kominos, D., Robertson, S. R., Pant, N., Baltimore, D., Birge, R. B., Cowburn, D., Hanafusa, H., Mayer, B. J., Overduin, M., Resh, M. D., Rios, C. B., Silverman, L., and Kuriyan, J. (1992) *Nature 358*, 646−653.
6. Waksman, G., Shoelson, S. E., Pant, N., Cowburn, D., and Kuriyan, J. (1993) *Cell 72*, 779−790.
7. Xu, W., Harrison, S. C., and Eck, M. J. (1997) *Nature 385*, 595−602.
8. Songyang, Z., Shoelson, S. E., Chaudhuri, M., Gish, G., Pawson, T., Haser, W. G., King, F., Roberts, T., Ratnofski, S., Lechleider, R. J., Neel, B. G., Birge, R. B., Fajardo, J. E., Chou, M. M., Hanafusa, H., Schaffhausen, B., and Cantley, L. C. (1993) *Cell 72*, 767−778.
9. Marengere, L. E., Songyang, Z., Gish, C. D., Schaffer, M. D., Parsons, J. T., Stern, M. J., Cantley, L. C., and Pawson, T. (1994) *Nature 369*, 502−505.
10. Songyang, Z., Gish, G., Mbamalu, G., Pawson, T., and Cantley, L. C. (1995) *J. Biol. Chem. 270*, 26029−26032.
11. Morelock, M. M., Ingraham, R. H., Betageri, R., and Jakes, S. (1995) *J. Med. Chem. 38*, 1309−1318.
12. Cousins-Wasti, R., Ingraham, R. H., Morelock, M. M., and Grygon, C. A. (1996) *Biochemistry 35*, 16746−16752.
13. Gilmer, T., Rodriguez, M., Jordan, S., Crosby, R., Alligood, K., Green, M., Kimery, M., Wagner, C., Kinder, D., Charifson, P., Hassel, A. M., Willard, D., Luther, M., Rusnak, D., Sternbach, D. D., Mehrotra, M., Peel, D., Shampine, L., Davis, R., Robbins, J., Patel, I. R., Kassel, D., Burkhart, W., Moyer, M., Bradshaw, T., and Berman, J. (1994) *J. Biol. Chem. 269*, 31711−31719.
14. Lemmon, M. A., and Ladbury, J. E. (1994) *Biochemistry 33*, 5070−5076.
15. Ladbury, J. E., Lemmon, M. A., Zhou, M., Green, J., Botfield, J., and Schlessinger, J. (1995) *Proc. Natl. Acad. Sci. U.S.A. 92*, 3199−3203.
16. Ladbury, J. E., Hensmann, M., Panayotou, G., and Campbell, I. D. (1996) *Biochemistry 35*, 11062−11069.
17. Lemmon, M. A., Ladbury, J. E., Mandiyan, V., Zhou, M., and Schlessinger, J. (1994) *J. Biol. Chem. 269*, 31653−31658.
18. McNemar, C., Snow, M. E., Windsor, W. T., Prongay, A., Mui, P., Zhang, R., Durkin, J., Le, H. V., and Weber, P. C. (1997) *Biochemistry 36*, 10006−10014.
19. Charifson, P. S., Shewchuck, L. M., Rocque, W., Hummel, C. W., Jordan, S. R., Mohr, C., Pacofsky, G. J., Peel, M. R., Rodriguez, M., Sternbach, D. D., and Consler, T. G. (1997) *Biochemistry 36*, 6283−6293.
20. Edelhoch, H. (1967) *Biochemistry 6*, 1948−1954.
21. Gill, S. C., and von Hippel, P. H. (1989) *Anal. Biochem. 182*, 319−326.
22. Rety, S., Futterer, K., Grucza, R. A., Munoz, C. M., Frazier, W. A., and Waksman, G. (1996) *Protein Sci. 5*, 405−413.
23. Pintar, A., Hensmann, M., Jumel, K., Pitkeathly, M., Harding, S. E., and Campbell, I. D. (1996) *Eur. Biophys. J. 24*, 371−380.
24. Wiseman, T., Williston, S., Brandts, J. F., and Lin, L.-N. (1989) *Anal. Biochem. 179*, 131−137.
25. Christensen, J. J., Hansen, L. D., and Izatt, R. M. (1976) *Handbook of proton ionization heats*, John Wiley & Sons, New York.
26. Murphy, K. P., Xie, D., Garcia, C., Amzel, L. M., and Freire, E. (1993) *Proteins: Struct., Funct., Genet. 15*, 113−120.
27. Richmond, T. J. (1984) *J. Mol. Biol. 178*, 63−89.
28. Wesson, L., and Eisenberg, D. (1992) *Protein Sci. 1*, 227−235.
29. Lee, B. K., and Richards, F. M. (1971) *J. Mol. Biol. 55*, 379−400.
30. Lesser, G. J., and Rose, G. D. (1990) *Proteins: Struct., Funct., Genet. 8*, 6−13.
31. Piccione, E., Case, R. D., Domchek, S. M., Hu, P., Chaudhuri, M., Backer, J. M., Schlessinger, J., and Shoelson, S. E. (1993) *Biochemistry 32*, 3197−3202.
32. Spolar, R. S., and Record, M. T. (1994) *Science 263*, 777−783.
33. Murphy, K. P., and Freire, E. (1992) *Adv. Protein Chem. 43*, 313−361.
34. Eftink, M., and Biltonen, R. (1980) in *Biological microcalorimetry*. (Beezer, A. E., Ed.) pp 343−412, Academic Press, London.
35. Ross, P. D., and Subramanian, S. (1981) *Biochemistry 20*, 3096−3102.
36. Lee, C. H., Kominos, D., Jacques, S., Margolis, B., Schlessinger, J., Shoelson, S. E., and Kuriyan, J. (1994) *Structure 2*, 423−438.
37. Pascal, S., Singer, A. U., Gish, G., Yamazaki, T., Shoelson, S. E., Pawson, T., Kay, L. E., and Forman-Kay, J. D. (1994) *Cell 77*, 461−472.
38. Rahuel, J., Gay, B., Erdmann, D., Strauss, A., Garcia-Echeverria, C., Furet, P., Caravatti, G., Fretz, H., Schoepfer, J., and Grütter, M. G. (1996) *Nat. Struct. Biol. 3*, 586−589.
39. Eck, M. J., Shoelson, S. E., and Harrison, S. C. (1993) *Nature 362*, 87−91.

BI973147K